SiO_2 content (in mol%) could possibly reduce the dipole–dipole interaction, leading to a reduction in the dielectric constant. Further, it is seen that the dielectric dispersion ($\Delta\varepsilon'$) which is the variation of dielectric constant (ε') over the measured frequency range (10 kHz–5 MHz; $\omega = 2\pi f$), is less than 3% at room temperature. It is interesting to note from Figure 1 and Table 1 that although an increase in total alkali content from 0.105 (LS31) to 0.192 mol% (LS33) could decrease ε_∞ from 14.73 to 7.76, the dielectric dispersion in the glasses studied remained within ± 3%. The present glass system with a low dielectric dispersion could be considered as a possible candidate for high-frequency applications.

It is seen from Figures 3 and 4 that the LS31 glass has less conductivity, while those for LS1 and LS33 are nearly the same. Table 3 presents the activation energies for the DC conduction (E_σ) and hopping processes (E_h) for the said glasses. The calculated value of E_σ (1.14 eV) using Anderson–Stuart structural model for the glass LS1, agrees well with that obtained experimentally (1.18 eV).

Dielectric constant BaO–PbO–SiO_2 glasses containing different amounts of Na^+ and K^+ ions varies between 7.0 and 14.5 with $\Delta\varepsilon < 3\%$. σ_{dc} and ω_h, and their activation energies (E_σ and E_h) were derived from the conductivity studies on three selected glasses, LS31, LS1 and LS33. E_σ (1.18 eV) calculated using Anderson–Stuart model for LS1 agrees well with that obtained experimentally (1.14 eV). Unlike the conventional mixed-alkali system which exhibits higher activation energy, in the present glass system it is found that E_σ and E_h for LS1 having nearly equal amounts of Na^+ and K^+ ions, are less compared to those for extreme glasses LS31 and LS33. The reason for this unusual behaviour observed in E_σ and E_h for the present glass system is thought to be due to complex effect of both the mixed-alkali effect and some structural changes occurring in the glass network by change in SiO_2 content.

1. Shrikhande, V. K., Mirza, T., Sawant, B. B., Sinha, A. K. and Kothiyal, G. P., Micro hardness measurements on lead silicate glass. *Bull. Mater. Sci.*, 1998, **21**, 493–497.
2. Shrikhande, V. K., Sudarsan, V., Kothiyal, G. P. and Kulshreshtha, S. K., ^{29}Si MAS NMR and micro hardness studies of some lead silicate glasses with and without modifiers. *J. Non-Cryst. Solids*, 2001, **283**, 18–26.
3. Ngai, K. L. and Leon, C., Relating macroscopic electrical relaxation to microscopic movements of the ions in ionically conducting materials by theory and experiments. *Phys. Rev. B*, 1999, **60**, 9396–9405.
4. Ingram, M. D., Ionic conductivity in glass. *Phys. Chem. Glasses*, 1987, **28**, 215–234.
5. Bunde, A., Ingram, M. D. and Maass, P., The dynamic structure model for ion transport in glasses. *J. Non-Cryst. Solids*, 1994, **172–174**, 1222–1236.
6. Balaya, P. and Goyal, P. S., A high temperature cell for dielectric relaxation studies. *Indian J. Pure Appl. Phys.*, communicated.
7. Anderson, O. L. and Stuart, D. A., Calculation of activation energy of ionic conductivity in silica glasses by classical methods. *J. Am. Ceram. Soc.*, 1954, **37**, 573–580.
8. Greaves, G. N. and Ngai, K. L., Reconciling ionic transport properties with atomic structure in oxide glasses. *Phys. Rev. B*, 1995, **52**, 6358–6380.
9. Patel, H. K. and Martin, S. W., Fast ionic conduction in $Na_2S+B_2S_3$ glasses: compositional contributions to nonexponentiality in conductivity relaxation in the extreme low alkali-metal limit. *Phys. Rev. B*, 1992, **45**, 10292–10300.

ACKNOWLEDGEMENTS. We thank Dr V. C. Sahni, Director, Physics Group, BARC and Dr J. V. Yakhmi, Head TP&PED, BARC for their interest and encouragement. Valuable technical assistance received from Mrs Shobha Manikandan is acknowledged.

Received 27 January 2003; revised accepted 30 September 2003

Sniffing a single molecule through SERS using Au_{core}–Ag_{shell} bimetallic nanoparticles

Madhuri Mandal[†], Subrata Kundu[†], Sujit Kumar Ghosh[†], Nikhil Ranjan Jana[‡], Mruganka Panigrahi[#] and Tarasankar Pal[†,*]

[†]Department of Chemistry, and [#]Department of Geology and Geophysics, Indian Institute of Technology, Kharagpur 721 302, India
[‡]Department of Chemistry and Biochemistry, University of Arkansas, Fayetteville, AR 72701, USA

In this communication we have described the preparation of a new class of core–shell type, i.e. Au_{core}–Ag_{shell} bimetallic nanoparticles by seed-mediated technique to examine the surface-enhanced Raman scattering (SERS) involving these particles. It has been demonstrated how the thickness of the Ag-shell could be tuned with the variation of gold seed to Ag-ion ratio with a view to examine the impact of the size and field effects of these bimetallics on SERS spectra. The sensitivity of the SERS detection limit has been improved down to the single molecular level through the formation of hot-particles due to aggregation of core–shell type particles in the presence of NaCl.

DETECTION and quantification of molecules has always been a challenge to a chemist. The greatest challenge is the state-of-the-art detection of a single molecule. Selective single-molecule detection using nanomaterials by surface enhanced Raman scattering (SERS) spectroscopy has currently shown new promise[1,2]. SERS spectroscopy was an accidental discovery by Fleischmann *et al.*[3]. SERS is a phenomenon by which Raman signals of nonresonant molecules adsorbed on noble metal particles are enhanced by 5 to 6 orders of magnitude[4,5]. In certain cases the enhancement is so enormous that it enables detection of a

*For correspondence. (e-mail: tpal@chem.iitkgp.ernet.in)

single molecule. During the course of investigation different 'hot particles' of metals have been synthesized whose roughened surface provides modest avenue for the adsorbed analyte to exhibit the resonance effect with the incoming laser beam. Although the theory of understanding the single-molecule SERS is at its infancy, two theories, chemical effect (CE) and electromagnetic effect (EM) exist to explain the SERS mechanism. Silver has been proved to be the best for the maximum enhancement of certain vibrational signals of an analyte. Keeping in view the existing theories and available information, we prepared Au_{core}–Ag_{shell} particles of different sizes (50 to 100 nm) with tunable Ag-shell thickness to get the advantages of CE and EM effects. These bimetallics become extremely efficient for surface optical enhancement, even better than monometallic Ag and Au nanoparticles. The particles in the ~50 nm size regime show best activity to enhance SERS signals. This communication may help us rationally design efficient and reproducible substrates for SERS spectroscopy by correlating particle size and optical enhancement.

First, gold seed particles of size ~15 nm were prepared by citrate-reduction procedure, as originally reported by Frens[6]. A 100 ml solution containing 0.01 g $HAuCl_4.3H_2O$ was heated to boiling, and then 3 ml of 1% sodium citrate solution was added to the boiling solution. The solution was further boiled for 1 h and the volume was made up to 100 ml by addition of water. The solution was cooled to room temperature. Here, the red-coloured gold particles were formed and these were used as seed (S) particles. From this 2.0, 1.0 and 0.5 ml of gold seed sol was taken in three different sets (A, B and C) respectively. Then $AgNO_3$ (0.001 mol dm^{-3}) was added to gold seed sol keeping the $AgNO_3$ concentration fixed for each set. Ascorbic acid (0.001 mol dm^{-3}) was used as the reducing agent and was added drop by drop under stirring condition. Total volume was made up to 10 ml for each set. Thus, by varying the proportion of gold seed to $AgNO_3$ and optimizing the synthetic condition, the thickness of silver shell was tuned to prepare the particles of different sizes such as ~50, ~70 and ~100 nm for the sets A, B and C respectively. By tuning the particle size it was possible to investigate the size effect on the SERS studies. The dye crystal violet (CV) in very low concentration (~10^{-8} to 10^{-11} mol dm^{-3}) was added to Au_{core}–Ag_{shell} particles of three different sizes (50, 70 and 100 nm) and kept for 2–3 h. This was incubated with NaCl and a droplet of 10 µl of this solution was spotted on a glass slide. The average radius of the drop became ~0.5 cm as the liquid spread over the slide. Renishaw Raman system 1000B coupled with a Leica DMLM microscope was used to screen the particles to investigate SERS activity. The SERS active nanoparticles were observed as bright spots. The Ar^{+} ion laser (λ= 514 nm) of 1.5 micron (µ) spot size was used to excite the CV molecules adsorbed on the nanoparticles.

The UV–visible spectra (Figure 1) authenticate the formation of Au_{core}–Ag_{shell} particles[7]. For gold seed particles (S) only the plasmon band appears with λ_{max} 525 nm, but for the core–shell structures (A, B and C), the plasmon bands appear with λ_{max} 425, 435 and 450 nm, which can exclusively be attributed to plasmon resonance of Ag particles present as shell. In case of core-shell type particles, a red shifting of the plasmon band was observed gradually as the seed concentration decreases from A to C, suggesting the formation of larger particles. A similar result was also observed by Wang *et al.*[8] and Jana *et al.*[9]. Moreover, the intensity of plasmon band for the different sets (A to C) varies with seed concentration, which suggests relatively smaller population of larger particles for lower seed concentration. Hence it is spelt out that optical properties of the core–shell nanoparticle are dominated by Ag-shell and the plasmon band is red-shifted as the Ag shell is gradually enlarged with the decrease in Au-seed concentration. From this we can infer that the reduction of Ag ion occurs on the surface of the preformed Au-core rather than forming more number of nucleation centres. As a result the Au_{core}–Ag_{shell} particles of different sizes were formed which has also been confirmed by comparing the experimental absorption spectra for these core–shell nanoparticles and their calculated spectra, according to the equation by Bohren and Huffmann[10]. The transmission electron micrograph of seed (S) and two representatives (A, B) of Au_{core}–Ag_{shell} type particles is shown in Figure 2. The EDX data again authenticate the formation of core–shell structure (Table 1). We exploit the particles to study the size effect for SERS enhancement. These particles have been shown to be SERS-active and the SERS spectra of CV molecules were obtained involving particles of different sizes. Reproducible SERS signals of the dye solutions (10^{-9} mol dm^{-3}) were obtained involving the particles. A surprising finding is that the particles having size in the

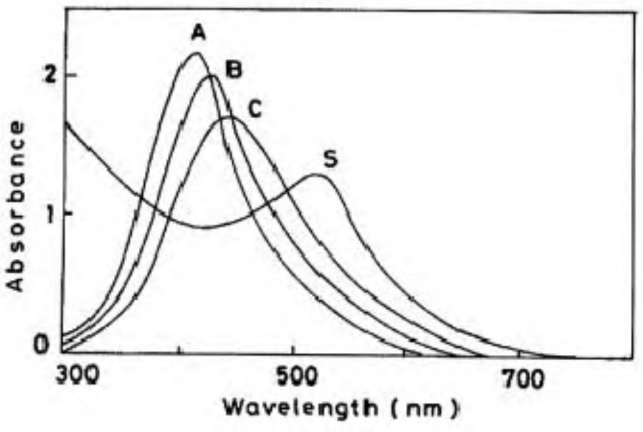

Figure 1. Plasmon absorption band corresponding to gold seed (S) and Au_{core}–Ag_{shell} particles (A, B and C) of ~50, 70 and 100 nm diameter respectively. Condition: 2.0, 1.0 and 0.5 ml of seed solution was used for A, B and C respectively. [$AgNO_3$] = 0.001 mol dm^{-3}, [ascorbic acid] = 0.001 mol dm^{-3} for all A, B and C.

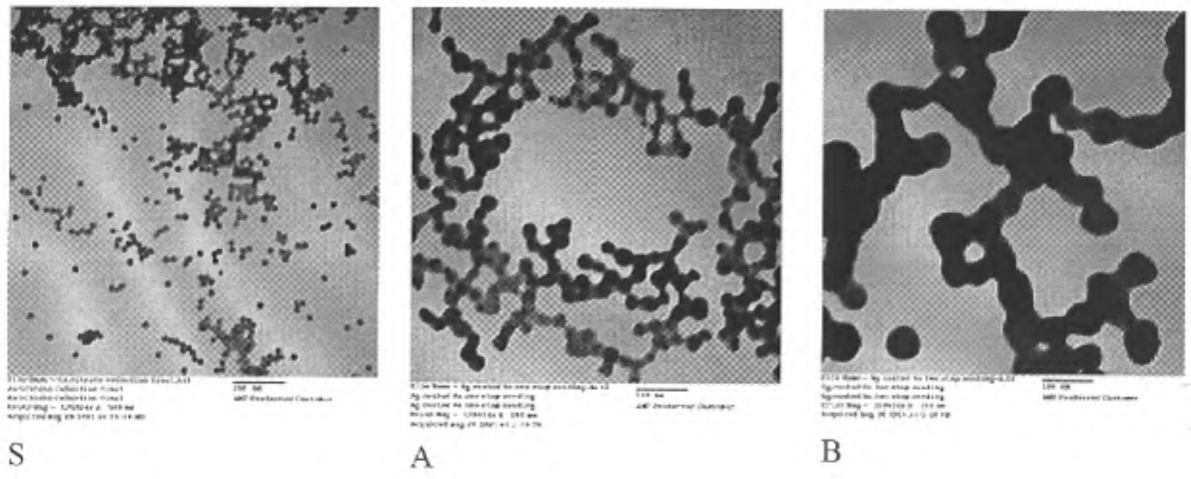

Figure 2. TEM images of seed (S) and Au_{core}–Ag_{shell} (A and B) of ~50 and 70 nm diameter respectively. Bar = 100 nm. Condition: Same as in Figure 1.

Table 1. Atomic composition of Ag and Au at edge and centre of three different particles of set A (EDX data)

Element	Atomic % at the edge	Atomic % at the edge	Atomic % at the edge	Atomic % at the centre	Atomic % at the centre	Atomic % at the centre
Ag	93.69	92.03	91.75	56.22	54.56	58.51
Au	6.31	7.97	8.25	43.78	45.44	41.49

range of ~50 nm have been observed to be most sensitive to SERS; this size happens to be much smaller than SERS-active silver[11] (~100 nm) and gold particles[12] (~65 nm). So we intended to study a single-particle Raman scattering with 50 nm nanoparticles and we were able to see the SERS spectra of the dye concentration down to 10^{-11} mol dm^{-3}. In case of the control experiment, taking monometallics (Ag and Au particles independently) as substrates, the signal intensity for the dye could not be obtained below 10^{-8} mol dm^{-3}. Considering the concentration of CV (10^{-10} mol dm^{-3}), here the detection limit was calculated as ~10–12 molecules within the 1.5 μ laser spot size. Therefore, it can be inferred that at CV concentration 10^{-11} mol dm^{-3}, it is possible to detect a single molecule. At such a low concentration, reproducible spectra were not obtained and blinking was observed. A prominent reproducible SERS spectrum of CV molecules was obtained up to the 10^{-10} mol dm^{-3} concentration, using 50 nm particles (Figure 3). Here, it is also observed that there is an important role for NaCl to obtain single-molecule SERS spectra. It is well known that the addition of low concentration of NaCl to the Ag colloid yields significant increase in SERS signals[13–15]. Since extinction spectra, TEM measurements have shown that such low quantities of NaCl do not cause any significant aggregation of the particles, and it has often been proposed that NaCl serves as 'activating agent'[13,14], yielding significant increase in SERS signals. This activation may occur either by generating unique 'SERS-active sites' on the nanocrystal or by stabilizing the adsorbed molecule[11,16]. To test the importance of added electrolyte, single-molecule SERS spectra for CV were recorded from solutions in the presence and absence of NaCl (Figure 3 *a*, *b*). Then the TEM pictures of the substrates present in those solutions were also taken. These results suggest that the aggregation of colloids is responsible for single-molecule SERS and the special site lies at the junction of two particles. As the two particles approach each other their transition dipoles, composed of oscillating and ballistic carriers in each particle couple and the coupled plasmon resonance shifts to the red region due to which the enhanced electromagnetic field increases at the junction between the particles. So the junction can function as an electromagnetic 'hot spot'[15]. As the dye molecules get adsorbed at the junction, it becomes highly SERS-active and is be able to give single-molecule SERS spectra. Figure 3 *c*–*f* shows four consecutive CV–SERS single-molecule spectra taken using ~8 mW laser power with 10 s integration times. The intense signals at 1172, 1217, 1366 and 1621 cm^{-1} correspond to Raman-active vibrational modes of CV adsorbed on the particle surface[12]. Relative intensities of Raman bands show fluctuations of approximately 25%. This is due to movement of the molecule into and out of the SERS active 'hot spots' or blinking of some single-molecule SERS signals[13,17].

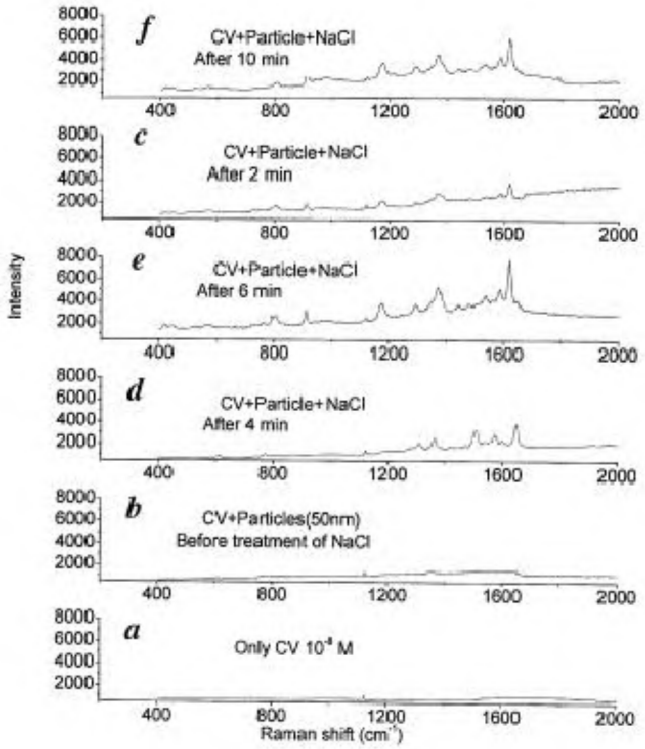

Figure 3. *a*, Raman spectra of aqueous solution of CV only. Condition: [CV] = 10^{-8} mol dm^{-3}; *b*, Raman spectra of CV adsorbed on 50 nm particle without treatment with NaCl; *c–f*, Single-molecule SERS spectra of CV adsorbed on the particles of 50 nm at various times on treatment with NaCl. Condition: [CV] = 10^{-10} mol dm^{-3}, [NaCl] = 0.01 mol dm^{-3}.

According to the Otto and Person models, to have single-molecule SERS, there should be extensive coupling between the adsorbed molecule and metallic surface[15]. This is possible due to increase in the Fermi energy level of the metal in the nano stage. This causes a decreased energy gap between the Fermi level of the nanoparticles and LUMO of the adsorbed molecules. Thus, at a certain level of Fermi energy, the HOMO–LUMO energy separation resonates with the Fermi level and respond to SERS. This effect is much more pronounced in the case of the reported 'core–shell' structures of 50 nm.

1. Moerner, W. E. and Orrit, M., Illuminating single molecules in condensed matter. *Science*, 1999, **283**, 1670–1676.
2. Xie, X. S. and Trautman, J. K., Optical studies of single molecules at room temperature. *Annu. Rev. Phys. Chem.*, 1998, **59**, 441–480.
3. Fleischmann, M., Hendra, P. J. and McQuillan, A. J., Raman spectra of pyridine adsorbed at a silver electrode. *Chem. Phys. Lett.*, 1974, **26**, 163–166.
4. Moskovits, M., Surface-enhanced spectroscopy. *Rev. Mod. Phys.*, 1985, **57**, 783–826.
5. Campion, A. and Kambhampati, P., Surface-enhanced Raman scattering. *Chem. Soc. Rev.*, 1998, **27**, 241–250.
6. Frens, G., Controlled nucleation for the regulation of the particle size in monodisperse gold suspensions. *Nature*, 1972, **241**, 20–22.
7. Mallik, K., Mandal, M., Pradhan, N. and Pal, T., Seed mediated formation of bimetallic nanoparticles by UV irradiation: A photochemical approach for the preparation of 'core-shell' type structure. *Nano Lett.*, 2001, **1**, 319–322.
8. Wang, H., Lu, L., Zhou, Y., Xi, S., Zhang, H., Hu, J. and Zhao, B., Seed-mediated growth of large, monodisperse core–shell gold–silver nanoparticles with Ag-like optical properties. *Chem. Commun.*, 2002, 144–145.
9. Jana, N. R., Gearheart, L. and Murphy, C. J., Evidence for seed-mediated nucleation in the chemical reduction of gold salts to gold nanoparticles. *Chem. Mater.*, 2001, **13**, 2313–2322.
10. Bohren, C. F. and Huffmann, D. F., *Absorption and Scattering of Light of Small Particles*, Wiley, New York, 1983, pp. 183–188.
11. Emory, S. R., Haskins, W. E. and Nie, S., Direct observation of size-dependent optical enhancement in single metal nanoparticles. *J. Am. Chem. Soc.*, 1998, **120**, 8009–8010.
12. Krug, II, J. T., Wang, G. D., Emory, S. R. and Nie, S., Efficient Raman enhancement and intermittent light emission observed in single gold nanocrystals. *J. Am. Chem. Soc.*, 1999, **121**, 9208–9214.
13. Michaels, A. M., Nirmal, M. and Brus, L. E., Surface enhanced Raman spectroscopy of individual Rhodamine 6G molecules on large Ag nanocrystals. *J. Am. Chem. Soc.*, 1999, **121**, 9932–9939.
14. Hildebrandt, P. and Stockburger, M., Surface-enhanced resonance Raman spectroscopy of Rhodamine 6G adsorbed on colloidal silver. *J. Phys. Chem.*, 1984, **88**, 5935–5944.
15. Michaels, A. M., Jiang, J. and Brus, L., Ag nanocrystal junctions as the site for surface-enhanced Raman scattering of single Rhodamine 6G molecules. *J. Phys. Chem. B*, 2000, **104**, 11965–11971.
16. Schneider, S., Grau, H., Halbig, P., Freunscht, P. and Nickel, U., Stabilization of silver colloids by various types of anions and their effect on the surface-enhanced Raman spectra of organic dyes. *J. Raman Spectrosc.*, 1995, **27**, 57–68.
17. Nie, S. and Emory, S. R., Probing single molecules and single nanoparticles by surface-enhanced Raman scattering. *Science*, 1997, **275**, 1102–1106.

ACKNOWLEDGEMENTS. We thank CSIR and DST, New Delhi for financial assistance.

Received 17 May 2003; revised accepted 6 January 2004

On the role of environment on corrosion resistance of the Delhi iron pillar

S. Halder, G. K. Gupta and R. Balasubramaniam*

Department of Materials and Metallurgical Engineering,
Indian Institute of Technology, Kanpur 208 016, India

The total wetting time of the Delhi iron pillar due to rainfall and atmospheric conditions has been estimated. The wetting of the Delhi iron pillar due to environmental conditions was estimated by applying a non-steady state heat-transfer mathematical model. The estimated wetting times due to environmental conditions were two orders of magnitude lower than due to rainfall. The predicted wetting times were used to estimate the anticipated rust thickness on the surface of the Delhi iron pillar. This was much higher than the actual rust thickness on the pillar. Therefore, the importance of the protective passive film mechanism of

*For correspondence. (e-mail: bala@iitk.ac.in)